

Analysis of cyclone separator solutions depending on SEC outlet conditions in nCO₂PP

Milad Amiri^{1*}, Pawel Ziolkowski¹, Kamil Stasiak¹, Dariusz Mikielwicz¹

¹ Faculty of Mechanical Engineering and Ship Technology, Gdańsk University of Technology,
ul. Gabriela Narutowicza 11/12, 80-233 Gdańsk, Poland

Corresponding Author:

milad.amiri@pg.edu.pl

Abstract

Utilization of spray ejector condenser in order to carry out direct-contact condensation of vapour with inert gas (CO₂) on a spray of subcooled liquid integrated with separator (to make pure CO₂) has been proposed for the task of condensation and CO₂ separation in the negative CO₂ emission gas power plant. Condensation and separation has a significant impact on the thermodynamic efficiency of the entire negative CO₂ emission gas power plant cycle. The study presents the accomplished analysis using the numerical model of cyclone separator cases with varying spray ejector condenser outlet conditions. The model incorporates the continuity and momentum equations to describe the phenomenon of separation. Here, transient, turbulent and three-dimensional separator is numerically modelled based on a control volume method in Fluent. The Reynolds Stress Model is also derived from Reynolds Averaged Navier-Stokes's solution. This model is adopted to numerically simulate turbulent flow in separators. In addition, the mixture model is applied for simulation of turbulent swirl two-phase flow in gas-liquid separator. To obtain a numerical model and optimize the purification of CO₂, firstly, different length of cone of cyclone separator should be investigated. Then, the numerical simulation on different value of volume fraction of two phase flow is conducted, and by applying 10% up to 20% of volume fraction for water liquid, the model is derived. Results show that as the liquid volume fraction decreases, the separation efficiency improves. The most optimal separation efficiency of 90.7% is achieved when the liquid volume fraction is at 10%. In addition, Increasing the length of the cone results in both higher efficiency and pressure drop. Specifically, when the length of the cone is increased from 128 mm to 528 mm, the efficiency and pressure drop increases by 4.2% and 194.14 (pa), respectively.

Keywords

CFD, Separator, Gas-liquid separation, Separation efficiency, Three-Dimensional

1. Introduction

Carbon dioxide is deemed to be a major contributor to global warming [1]. Given the substantial effect of CO₂ on climate change, various methods have been devised in recent years to manage carbon emissions, including CO₂ capture [2] and storage [3]. Generating electricity with negative CO₂ emissions is achievable through a new concept that involves oxy-combustion in a wet combustion chamber, followed by separation of water and CO₂ through a compact spray ejector condenser (SEC), and finally compression of the separated CO₂. The developed cycle of a negative CO₂ emission power plant includes some devices, out of which, spray ejector condenser as well as separator plays an indispensable role to make pure CO₂. Figure 1 depicts the process flow diagram (PFD) of the negative CO₂ emission gas power plant [4, 5]. As it can be seen in Fig.1b, separation unit consists of SEC and cyclone separator. The main task of SEC is to condense the water vapour from the exhaust gases while maintaining a compact system structure, so that it has two inlets (for suction fluid and motive fluid) and one outlet. At the SEC outlet, the water liquid and CO₂ are expected to enter the cyclone separator for purification of CO₂.

Cyclones are widely utilized in industries including mineral, chemical, environmental and petroleum engineering for separating gas from solids or liquids [6, 7]. The performance of a cyclone separator is influenced by various factors including its structure geometry and operational parameters [8]. Studies have also been investigated on the impact of a cone that is extended with a vertical tube on the efficiency of a cyclone separator [9, 10]. The effects of cone and cylinder length on separation efficiency and pressure drop have been investigated by Brar et al. [11] and Prasanna et al. [12].

In this paper, the SEC and cyclone separator are considered a novel separation process to purify CO₂, which has not been extensively studied in previous literature. Therefore, a tangential-flow CO₂-water separator was designed to obtain the desired high-purity CO₂ flow for the Negative CO₂ Emission Gas Power Plant (nCO₂PP) [13]. To obtain a numerical model and optimize the performance of separator, firstly, the effect of cone size should be defined. Then, a suitable value of liquid volume fraction depending on conditions of spray ejector condenser can be obtained using separation efficiency, so that the numerical simulation on different value of volume fraction of water liquid is conducted, and by applying 10% up to 20% of volume fraction for water liquid, the model is derived.

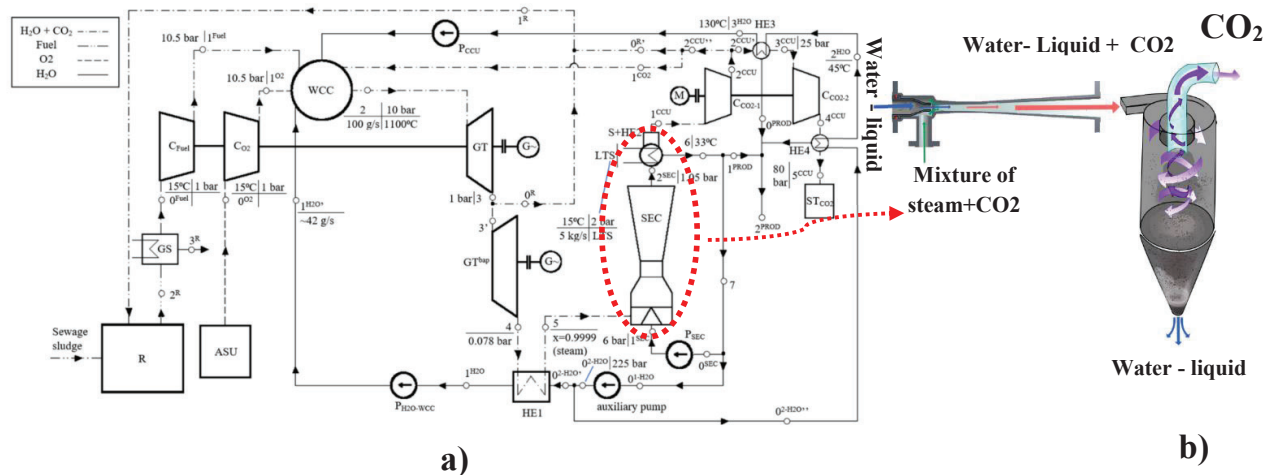


Figure. 1. a) Negative CO₂ emission gas power plant process flow diagram (PFD), b) Capturing CO₂ part consist of spray ejector condenser (SEC) and cyclone separator [4, 5]

2. Modeling

The effectiveness of a cyclone separator is influenced by various factors, and optimal separation efficiency and reduced pressure loss can only be achieved when the dimensions of its components are suited to the purpose. The tangential inlet type is widely adopted in industries and is considered mature with a simple structure typically consisting of a cylinder and cone section. Figure 2a shows the geometry of a three-dimensional tangential inlet cyclone separator. CO₂-Water mixture enters the separator with high velocity in a tangential direction and rotates rapidly in the annular space between the exhaust pipe and cylinder. Under the influence of centrifugal force, the water droplets in the mixture are hurled to the wall and then fall down along the wall due to the gravity and momentum of the mixture. Afterward, they are discharged through the underflow outlet. The purified CO₂ travels upward through the center and discharges through the exhaust pipe. The dimensions of three-dimensional tangential single inlet cyclone separator have been indicated in Fig 2b and table 1.

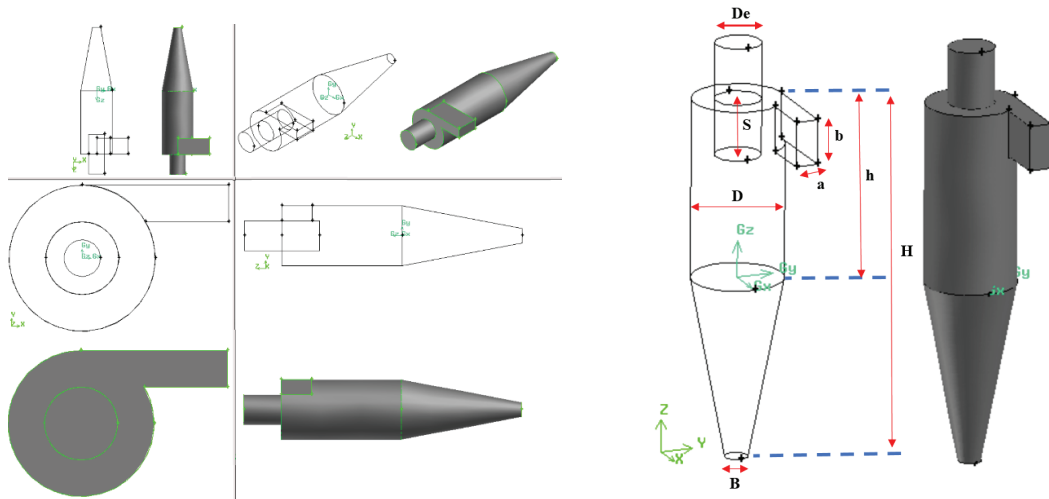


Figure 2. a) Geometry of the cyclone separator seen from different views and b) its dimensions

Table 1. Dimensions of the cyclone ($D = 0.2$ m)

| $\frac{a}{D}$ | $\frac{b}{D}$ | $\frac{De}{D}$ | $\frac{S}{D}$ | $\frac{h}{D}$ | $\frac{H}{D}$ | $\frac{B}{D}$ |
|---------------|---------------|----------------|---------------|---------------|---------------|---------------|
| 0.25 | 0.5 | 0.5 | 0.625 | 2 | 4 | 0.25 |

a)

b)

2.1. Governing equations

In this study, we applied the mixture model, also known as the algebraic slip model, a simplified version of the Euler-Euler approach. This model is appropriate for bubbly, droplet, or particle-laden flows where the volume fraction of the dispersed phase is high enough (>10%), to ensure pronounced inter-particle collision. The mixture model allows fluid phases to flow at different velocities and permits fluid phases to penetrate each other, and enables the exchange of mass, momentum, and energy between fluid phases. The mixture model has also been used in CFD simulations of turbulent swirl two-phase flow in gas-liquid cyclone separators.

However, the calculation for the continuous and dispersed fluid phases is performed through the following methods: The Reynolds-averaged Navier-Stokes, continuity, and momentum equations are used to solve for the continuous phase.

$$\frac{\partial \rho}{\partial t} + \frac{\partial(\rho u_i)}{\partial x_i} = 0 \quad (1)$$

$$\frac{\partial(\rho u_i)}{\partial t} + \frac{\partial(\rho u_i u_j)}{\partial x_j} = \frac{\partial P}{\partial x} + \frac{\partial}{\partial x} \left(\mu \frac{\partial^2 u_i}{\partial x_j^2} + \frac{\partial^2 u_j}{\partial x_i^2} - \frac{2}{3} \delta_{ij} \frac{\partial u_k}{\partial x_k} + \frac{\partial}{\partial x_j} \right) (-\rho \overline{u_i u_j}) \quad (2)$$

$$(-\rho \overline{u_i u_j}) = \mu_t \left(\frac{\partial^2 u_i}{\partial x_j^2} + \frac{\partial^2 u_j}{\partial x_i^2} \right) - \frac{2}{3} (\rho k + \mu_t \frac{\partial u_k}{\partial x_k}) \delta_{ij} \quad (3)$$

The equation for the continuity of the mixture can be calculated as:

$$\frac{\partial(\rho_m)}{\partial t} + \frac{\partial(\rho_m u_m)}{\partial x_i} = 0 \quad (4)$$

Mixture momentum:

$$\frac{\partial(\rho_m u_{mi})}{\partial t} + \frac{\partial(\rho_m u_{mi} u_{mj})}{\partial x_i} = \frac{\partial P}{\partial x_i} + \frac{\partial}{\partial x_j} \mu_m \left(\frac{\partial u_{mi}}{\partial x_j} + \frac{\partial u_{mj}}{\partial x_i} \right) + \rho g_i + \frac{\partial}{\partial x_i} \left(\sum_{q=1}^n \alpha_q \rho_q u_{dr,qi} u_{dr,qj} \right) \quad (5)$$

Where u_m is the mass-averaged velocity, ρ_m is the mixture density and μ_m is the viscosity of the mixture.

$$U_m = \frac{\sum_{q=1}^n \alpha_q \rho_q u_q}{\rho_m}, \rho_m = \sum_{q=1}^n \alpha_q \rho_q, \mu_m = \sum_{q=1}^n \alpha_q \mu_q \quad (6)$$

Where $u_{dr,q}$ represents the drift velocity for secondary, calculated as $u_{dr,q} = u_q - u_m$.

In the RSM with a time step of 0.001 (s), the equation for transport is formulated as follows.

$$\frac{\partial}{\partial t} (\rho \overline{u'_i u'_j}) + \frac{\partial}{\partial x_k} (\rho u_k \overline{u'_i u'_j}) = D_{ij} + P_{ij} + \Pi_{ij} + \varepsilon_{ij} + S \quad (7)$$

where the two terms on the left side represent the local time derivative of stress and the convective transport term, respectively. The five terms on the right side are:

$$\text{The stress diffusion term: } D_{ij} = -\frac{\partial}{\partial x_k} \left[\overline{\rho u'_i u'_j u'_k} + \overline{(P' u'_j)} \delta_{ik} + \overline{(P' u'_i)} \delta_{jk} - \mu \left(\frac{\partial}{\partial x_k} \overline{u'_i u'_j} \right) \right] \quad (8)$$

$$\text{the shear production term: } P_{ij} = -\rho \left[\overline{u'_i u'_k} \frac{\partial u_j}{\partial x_k} + \overline{u'_j u'_k} \frac{\partial u_i}{\partial x_k} \right] \quad (9)$$

$$\text{The pressure-strain term: } \Pi_{ij} = p \left(\frac{\partial u'_i}{\partial x_j} + \frac{\partial u'_j}{\partial x_i} \right) \quad (10)$$

$$\text{The dissipation term: } \varepsilon_{ij} = -2\mu \frac{\partial u'_i}{\partial x_k} \frac{\partial u'_j}{\partial x_k} \quad (11)$$

$$\text{and the source term: } S \quad (12)$$

2.2. Numerical simulation and boundary conditions

As it mentioned the CO₂-water multiphase flow in the cyclone separator was accurately modeled using the multiphase mixture model in ANSYS Fluent 2021 R1. This was deemed necessary as the CO₂ and water phases are expected to have a strong interaction within the swirling environment of the cyclone separator. In the interpenetrating continuum, CO₂ was the primary (continuous) phase and water was the secondary (dispersed) phase and surface tension was considered. The SIMPLE algorithm was applied to establish the coupling between the pressure and velocity in the continuity and momentum equations. PRESTO scheme was considered for its superior performance in estimating high-speed swirling flows and flows in curved domains. The momentum, volume fraction, and kinetic energy equations were discretized using the QUICK method, which provides more accurate results for rotational swirling flows compared to first- and second-order schemes due to its higher-order discretization. The first-order discretization can result in higher error and unreliable results [14]. The boundary conditions are presented in Table 2.

Table 2. Boundary conditions

| Boundary | Types |
|----------|----------------|
| Inlet | Velocity inlet |
| Outlets | Outflow |
| Wall | No Slip wall |

3. Evaluation of numerical model

The ANSYS Fluent 2021 R1 was used to evaluate the flow pattern of the studied cyclone separator. As a preliminary parameter, the separation efficiency was calculated, which was defined as follows:

$$\eta = \left(\frac{\dot{m}_{liquid\ at\ inlet} - \dot{m}_{liquid\ at\ gas\ outlet}}{\dot{m}_{liquid\ at\ inlet}} \right) \times 100 \quad (13)$$

Where \dot{m} is the mass flow rate.

3.1 Grid Independence

The geometry and mesh of the cyclone separator created in Gambit 2.4.6 are shown in Fig. 3. To ensure accuracy in calculations, all edges were meshed in the created model. Following that, all the faces and volumes were meshed. For the purpose of meshing, the Tet/Hybrid elements and TGrid type were employed to create cells appropriate for the geometry involved in computational fluid dynamics (CFD) simulations. A high-quality mesh was crucial to avoid errors caused by numerical diffusion. Thus, mesh-independent solutions for the cyclone separator were verified using different grids. So, to examine the independence of the results from the grid size, the variation of tangential velocity and separation efficiency versus different nodes is shown in Fig 4. As it can be seen, the results of 40574 and 80974 grids are different from other grids (120654 and 160214). Even though the 120654 and 160214 consequences are approximately the same, in order to lower computational cost, the 120654 nodes have been opted.

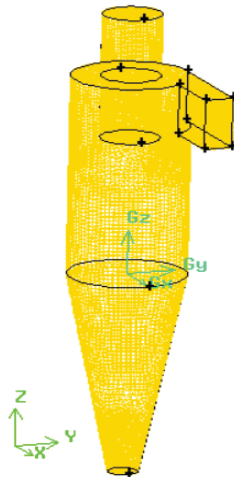


Figure 3. Meshing of cyclone separator

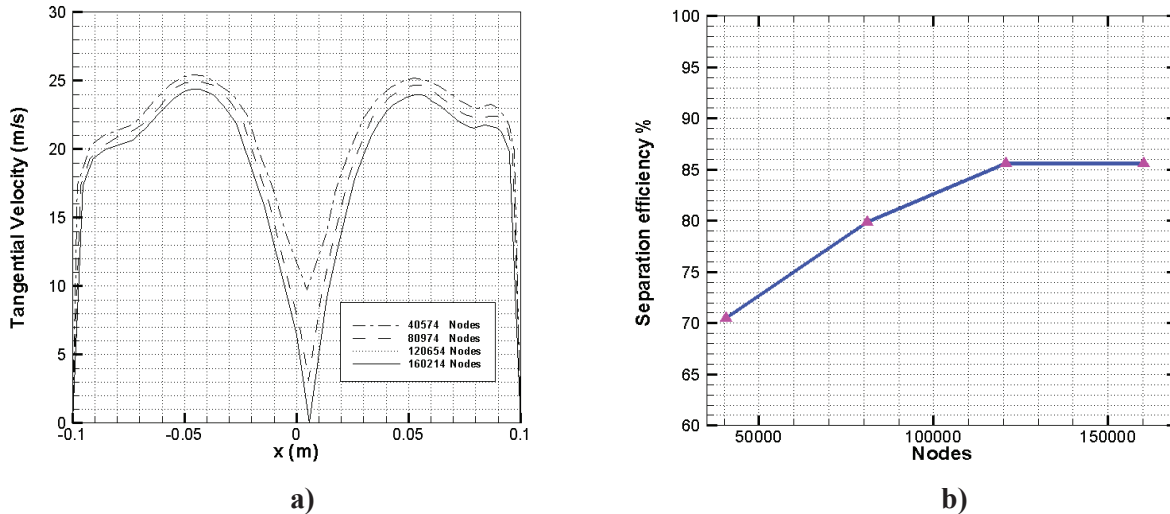


Figure 4. Grid independency for a) Tangential velocity and b) separation efficiency of single inlet cyclone at $2.8 \left(\frac{kg}{s}\right)$ when volume fraction of water is 10%

3.2 Model Validation

Figure 5. shows predicted variation of the Pressure drop, tangential velocity and separation efficiency in comparison to the results of Wang et al [15]. In their physical experiment, air was fed into the inlet of the cyclone, and its flow rate was monitored using a flowmeter. The velocity of both phases was set at 20 m/s. The outlet tube was open to the atmosphere and the gas pressure at the top of the vortex finder was maintained at 1 atm. The volume fraction of the second phase was 10%. The measurement of velocity and pressure in the gas field was performed using a five-hole probe, which comprised an adjustable frame and five pressure transducers. The voltage signals generated by the five pressure transducers on the five-hole probe were amplified after being placed in the gas flow field. The amplified voltage signals were collected by a data acquisition system equipped with a

microprocessor and a personal computer. As it can be seen in Fig 5. good agreement was achieved between the experimental and the numerical results data taken from the studies by Wang et al.

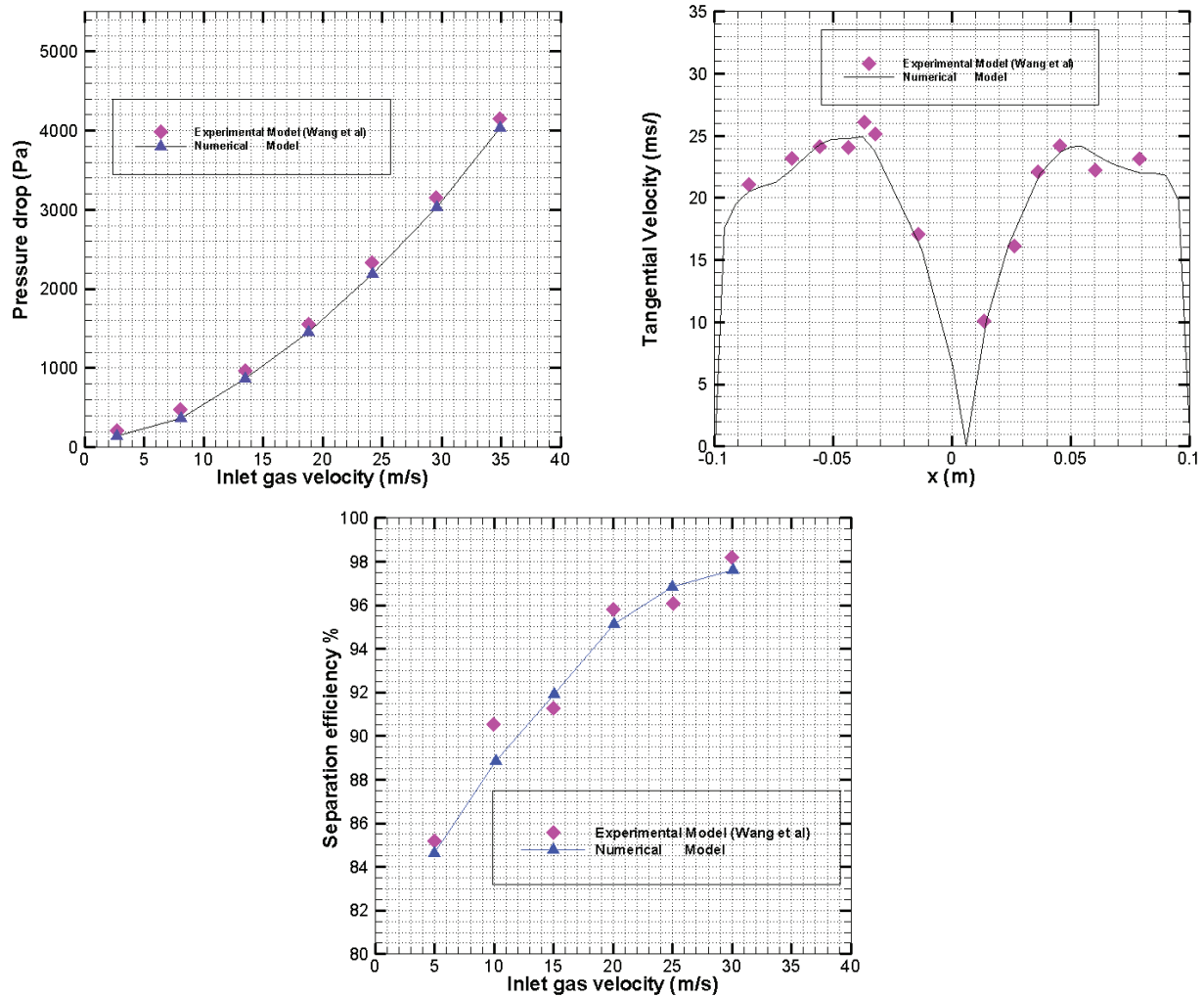


Figure. 5. Pressure drop, tangential velocity and separation efficiency comparison of experimental model (Wang et al) and current simulation

4. Results and discussion

4.1 Effect of cone size

The design and operation of a cyclone separator is crucial in determining the efficiency of particle separation in various industrial applications. One of the design parameters that affects the performance of the cyclone separator is the size of cone. Figure 6 depicts geometry and mesh of cyclones with different cone length. In this section, the effect of cone size (at constant total length of cyclone: 638 (mm)) on the efficiency and pressure drop of a cyclone

separator has been examined (Table.3). The results indicate that while the efficiency of the cyclone increases with a longer cone, there is also a corresponding increase in pressure drop

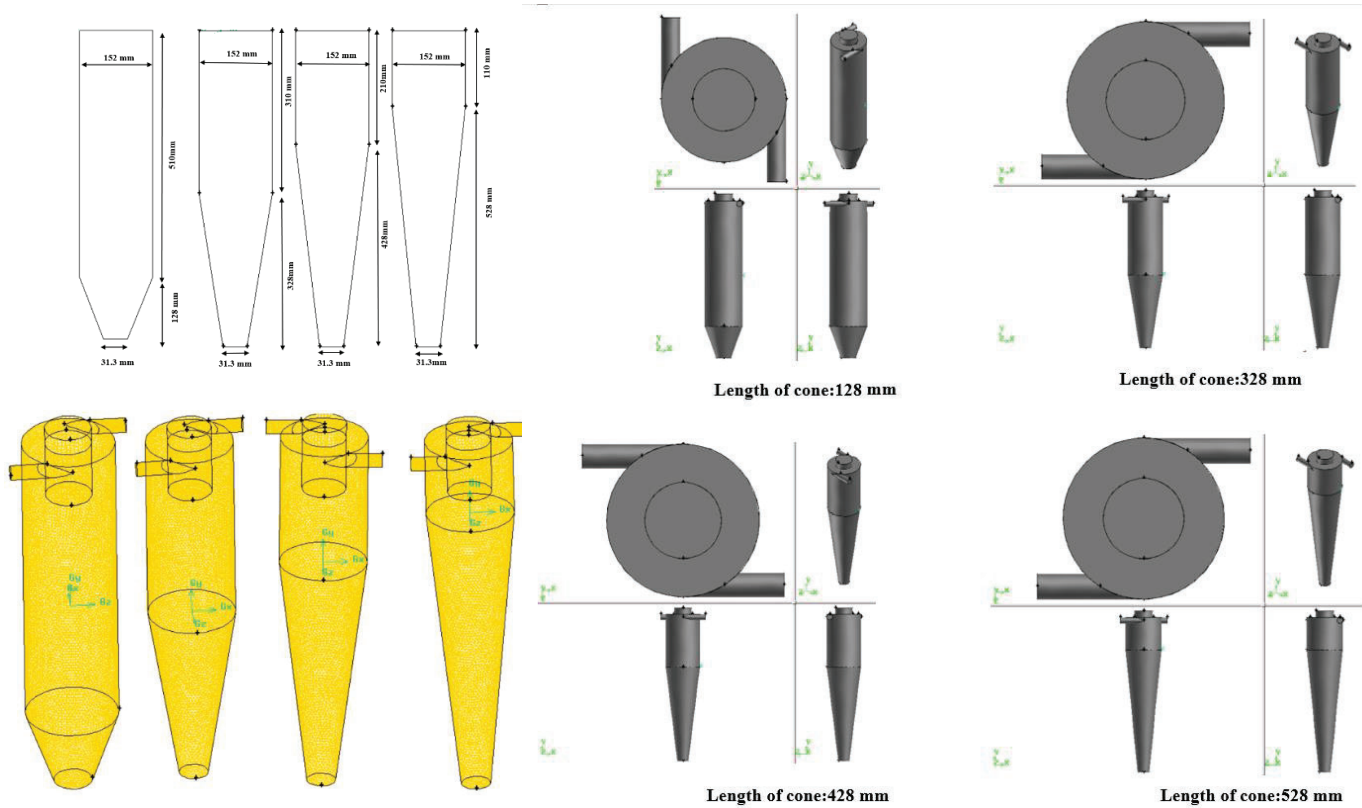


Figure.6. Geometry and mesh of cyclones with different cone length

Table 3. Mass flow rate of liquid phase at the inlet and gas outlet for different length of cone at 10% of liquid volume fraction and diameter of water droplet : $10\ (\mu m)$

| Length of Cone (mm) | $\dot{m}_{liquid\ at\ inlet}$ (kg/s) | $\dot{m}_{liquid\ at\ gas\ outlet}$ (kg/s) | Efficiency % | Pressure drop (Pa) |
|---------------------|--------------------------------------|--|--------------|--------------------|
| 128 | 0.43527386 | 0.14555562 | 66.5 % | 514.62 |
| 328 | 0.43527386 | 0.136807 | 68.6 % | 556.62 |
| 428 | 0.43527386 | 0.13143237 | 69.8 % | 622.66 |
| 528 | 0.43527386 | 0.12750024 | 70.7 % | 706.76 |

4.2 Efficiency of cyclone separator depending on SEC outlet conditions

When a saturated vapour contacts subcooled drops with a size larger than the critical value, the condensation occurs. Following our previous analytical model [16, 17], it is assumed that the inlet properties of the fluids are

supplied at a state denoted as "inlet" in Figure 7. To calculate the suction mass (m_g) and pressure at the beginning of the mixing zone, knowledge of the equations resulting from the flow in the inlet zone is required.

$$m_g = u_{gin}\rho_g A_{gin} = u_{g0}\rho_g(A_0 - A_l) \quad (14)$$

From Bernoulli equation:

$$p_{g,in} + \frac{1}{2} \cdot \rho_{g,0} u_{g,in}^2 = p_{g,0} + \frac{1}{2} \cdot \rho_{g,0} u_{g,0}^2 + \Delta p_{loss,1} \quad (15)$$

The suction pressure ($p_{g,1}$) generated by the liquid jet mixing with gases can be calculated by balancing the momentum between the pre-mixing section and the entrance to the mixing section, which corresponds to states 0 and 1.

$$p_{g,0}A_{g,0} + m_g u_{g,0} + p_l A_l + m_l u_l = p_{g,1}A_1 + (m_g + m_l)u_l \quad (16)$$

To obtain the values in state 2, the conservation equations for mass, energy, and momentum were applied simultaneously for the adiabatic process. When a non-condensable gas (CO_2) is present in the condensation space, it is necessary to analyse both heat and mass transfer. Based on the equations used in our previous analytical study [16, 17], condensation of vapour on subcooled droplet stream, heat balance of droplet stream and balance of mass and heat for vapour-gas mixture have been considered.

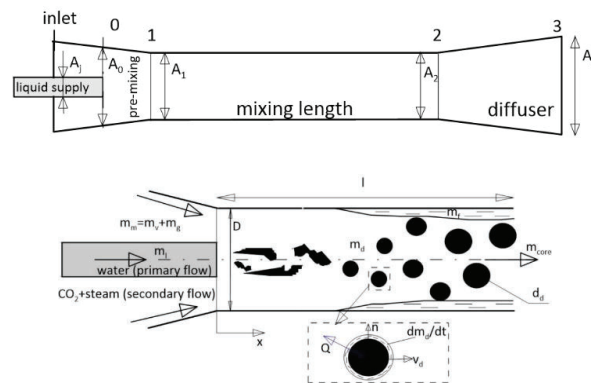


Figure 7. Schematic of the spray ejector of condenser [16, 17]

4.2.1 Effect of volume fraction

As mentioned above, spray ejector condenser and cyclone separator have been used as a separation section of a negative CO_2 emission power plant in regard to making pure CO_2 . Two choking phenomena exist in the ejector performance: one in the primary flow through the nozzle and the other in the entrained or suction flow (due to acceleration of the entrained flow from a stagnant state at the suction port to a supersonic flow in the mixing chamber). In addition, a jet coming out of the nozzle dissipates and breaks up into various-sized drops. The liquid stream breaks into droplets under the influence of waves formed on the surface of the stream due to instability. These waves cause a loss of stability and the formation of primary droplets. Secondary droplet breakup occurs under the influence of aerodynamic forces. Primary droplets are deformed and broken up by aerodynamic drag forces and surface tension forces.

So, according to aforementioned effects, volume fraction of water liquid will be different. This section presents the accomplished analysis using the numerical model of cyclone separator cases with varying SEC outlet conditions. To this end, 10%, 15% and 20% of volume fraction of water liquid have been considered. Figure 8 indicates the contour of volume fraction of water liquid for dual inlet cyclone at $2.8 \left(\frac{kg}{s}\right)$ inlet mass flow rate for 10%, 15% and 20% feed stream liquid volume fraction.

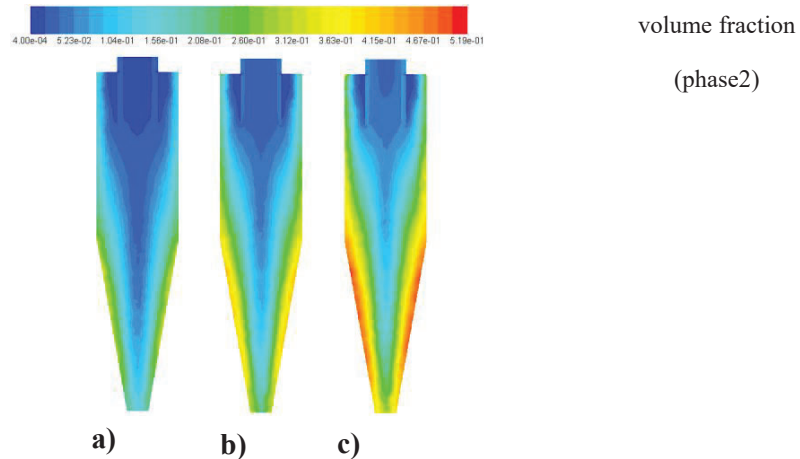


Figure 8. The contours volume of liquid fraction for $2.8 \left(\frac{kg}{s}\right)$ inlet mass flow rate, at feed stream liquid volume fraction a) 10%, b) 15 % and c) 20%

To assess the impact of liquid volume fraction on the internal configuration separation performance, the separation efficiency was computed at various volume fractions using Equation 13, and the results were compared. The separation efficiencies, inlet and outlet liquid mass flow rates (\dot{m}) at the considered three liquid volume fractions are shown in Table 4. As seen in the table, separation efficiency increases with decreasing liquid volume fraction, so that the maximum separation efficiency has been obtained at 10% of liquid volume fraction and its value is 90.7%.

Table 4. Separation efficiency of dual inlet cyclone at different volume fraction of water liquid when diameter of water droplet is 10^{-5}

| Liquid Volume Fraction | $\dot{m}_{liquid\ at\ inlet}$ (kg/s) | $\dot{m}_{liquid\ at\ gas\ outlet}$ (kg/s) | Separation efficiency, $\eta\%$ |
|------------------------|---|---|------------------------------------|
| 10 % | 2.74649 | 0.254949 | 90.7 % |
| 15 % | 4.1197319 | 0.43964297 | 89.33 % |
| 20 % | 5.4929759 | 0.68230528 | 87.58 % |

5. Conclusion

A numerical simulation was conducted to optimize the performance of a tangential-flow vanes CO₂-water separator design in Negative CO₂ Emission Power Plant (NCO₂PP) in regard to producing high-purity CO₂, using a transient RSM turbulent model and a three-dimensional model.

The key findings are summarized as follows:

- ❖ Increasing the cone length leads to elevated efficiency and pressure drop.
- ❖ The cone length is extended from 128 mm to 528 mm, the efficiency and pressure drop increase by 4.2% and 194.14 pa, respectively.
- ❖ Separation efficiency improves as the liquid volume fraction decreases, with the highest efficiency of 90.7% achieved at a liquid volume fraction of 10%.

For future research, the proposed model will be experimentally tested using single and multi-nozzle configurations to generate the motive fluid jets. Additionally, electro hydrodynamic (EHD) effects can be used to enhance heat transfer in direct contact condensation in spray ejector condensers. EHD is a process that involves the interaction between electric fields and fluid flow. In direct contact condensation, EHD can be used to create an electrostatic field that enhances the droplet size distribution, which leads to improved heat transfer. One way to implement EHD in spray ejector condensers is to use a corona discharge to create an electric field that attracts the charged droplets towards the condenser surface. This increases the surface area available for heat transfer and also increases the mass transfer rate between the droplets and the condenser surface. Another way to use EHD in spray ejector condensers is to apply a voltage to the ejector nozzle. This can cause the liquid droplets to break up into smaller droplets, which increases the surface area available for heat transfer and also enhances the mass transfer rate. So, it is aimed to impose EHD in spray ejector condenser which results in significant improvements in heat transfer efficiency and can also reduce the overall size of the condenser. Moreover, a quadruple inlet cyclone separator will be used to purify CO₂.

Acknowledgements

The research leading to these results has received funding from the Norway Grants 2014–2021 via the National Center for Research and Development. Article has been prepared within the frame of the project: “Negative CO₂ emission gas power plant” - NOR/POLNORCCS/NEGATIVE-CO₂- PP/0009/2019–00 which is co-financed by programme “Applied research” under the Norwegian Financial Mechanisms 2014–2021 POLNOR CCS 2019 - Development of CO₂ capture solutions integrated in power and industry processes.

| Nomenclature | | | |
|--------------|--|---------------------|---|
| D_j | diameter of jet, m | ρ | Density, (kg/m ³) |
| D_{ij} | stress diffusion term, kg/(ms ²) | ρ_m | mixture density, (kg/m ³) |
| D_0 | diameter of mixing length, m | μ_m | viscosity of the mixture, kg/(ms) |
| d_d | diameter of droplet, m | Π_{ij} | pressure-strain term, kg/(ms ²) |
| l | mixing length, m | μ_l | dynamic viscosity, kg/(ms) |
| m_g | suction mass, kg/s | | |
| n | total number of droplet | ε_{ij} | dissipation term, (kg/ms ³) |
| P | static Pressure, pa | η | separation efficiency, (%) |
| P_{ij} | shear production term, N/(m ³) | σ_l | surface tension, N/m |
| $p_{g,1}$ | suction pressure, pa | $\Delta p_{loss,1}$ | pressure drop, pa |

| | |
|----------------------|--------------------------------------|
| Re | Reynolds number |
| S | source term |
| \vec{u} | velocity vector, m/s |
| $u_{dr,q}$ | drift velocity for secondary, m/s |
| We | Weber number |
| Greek Symbols | |
| ρ_l | liquid density, kg/(m ³) |

References:

- [1] Pelletier C., Rogaume Y., Dieckhoff L., Bardeau G., Pons M-N., Dufour A. Effect of combustion technology and biogenic CO₂ impact factor on global warming potential of wood-to-heat chains. *Applied Energy*. 2019;235:1381-8.
- [2] Zhang Y., Gao Y., Louis B., Wang Q., Lin W. Fabrication of lithium silicates from zeolite for CO₂ capture at high temperatures. *Journal of energy chemistry*. 2019;33:81-9.
- [3] Lee E., Hornafius JS., Dean E., Kazemi H. Potential of Denver Basin oil fields to store CO₂ and produce Bio-CO₂-EOR oil. *International Journal of Greenhouse Gas Control*. 2019;81:137-56.
- [4] Ziółkowski P., Madejski P., Amiri M., Kuś T., Stasiak K., Subramanian N., et al. Thermodynamic analysis of negative CO₂ emission power plant using Aspen Plus, Aspen Hysys, and Epsilon software. *Energies*. 2021;14(19):6304.
- [5] Ziółkowski P., Stasiak K., Amiri M., Mikielwicz D. Negative carbon dioxide gas power plant integrated with gasification of sewage sludge. *Energy*. 2023;262:125496.
- [6] Yang J., Liu C., Li S., Sun B., Xiao J., Jin Y. A new pressure drop model of gas–liquid cyclone with innovative operation mode. *Chemical Engineering and Processing: Process Intensification*. 2015;95:256-66.
- [7] Safikhani H., Mehrabian P. Numerical study of flow field in new cyclone separators. *Advanced Powder Technology*. 2016;27(2):379-87.
- [8] Han C., Hu Y., Li W., Bie Q. Gas-solid separation performance and structure optimization in 3D printed guide vane cyclone separator. *Advanced Powder Technology*. 2022;33(11):103815.
- [9] Qian F., Zhang J., Zhang M. Effects of the prolonged vertical tube on the separation performance of a cyclone. *Journal of hazardous materials*. 2006;136(3):822-9.
- [10] Kaya F., Karagoz I. Numerical investigation of performance characteristics of a cyclone prolonged with a dipleg. *Chemical Engineering Journal*. 2009;151(1-3):39-45.
- [11] Brar LS., Sharma R., Elsayed K. The effect of the cyclone length on the performance of Stairmand high-efficiency cyclone. *Powder Technology*. 2015;286:668-77.
- [12] Prasanna N., Subramanian K., Ajay S., Rajagopal T., Vigneshwaran V. CFD study on the performance of reducing pressure drop holes in cyclone separator. *Materials Today: Proceedings*. 2021;43:1960-8.
- [13] Available from: <https://nco2pp.mech.pg.gda.pl/pl>.
- [14] Utikar R., Darmawan N., Tade M., Li Q., Evans G., Glennly M., et al. Hydrodynamic simulation of cyclone separators. *Computational fluid dynamics: InTech*; 2010. p. 241-66.
- [15] Wang B., Xu D., Chu K., Yu A. Numerical study of gas–solid flow in a cyclone separator. *Applied Mathematical Modelling*. 2006;30(11):1326-42.
- [16] Mikielwicz D., Amiri M., Mikielwicz J. A Simple Analytical Model of Direct-Contact Condensation from Vapour-Inert Gas Mixture in a Spray Ejector Condenser. Available at SSRN 4147312.
- [17] Mikielwicz D., Amiri M., Mikielwicz J. Direct-contact condensation from vapour-gas mixture in a spray ejector condenser for negative CO₂ power plant. 2nd International Conference on Negative CO₂ Emissions; 2022, Chalmers University of Technology, June 14-17.